

Magnetic instability of MgB₂ thin film triggered by the various sweeping rates of an applied magnetic field

Jae-Yeap Lee,¹ Hu-Jong Lee,¹ Myung-Hwa Jung,² Sung-Ik Lee,^{2,a)} Eun-Mi Choi,³ and W. N. Kang³

¹Department of Physics, Pohang University of Science and Technology, Pohang 790-784, Republic of Korea

²Department of Physics, National Creative Research Initiative Center for Superconductivity, Sogang University, Seoul 121-742, Republic of Korea

³Department of Physics and BK21 Division, Sungkyunkwan University, Suwon 440-746, Republic of Korea

(Received 7 October 2009; accepted 24 November 2009; published online 5 January 2010)

Up to now, the vortex avalanche is known to depend critically on the changing of some external parameters, such as the applied magnetic field, the temperature, and the demagnetization factor. In this study, we found the sweeping rate (SR) of the applied magnetic field to be another parameter that contributed to the appearance of the vortex avalanche. For example, a fast SR 500 Oe/s enhanced the vortex avalanche quietly compared to the case of a slow SR of 3 Oe/s. The dependence of the appearance of the vortex avalanche on the SR was quite strong, especially at low temperatures. A H - T phase diagram that distinguishes the regions of magnetic stability and instability is drawn for each SR. © 2010 American Institute of Physics. [doi:10.1063/1.3275913]

I. INTRODUCTION

In nature, quite a number of avalanches, such as snow avalanche and forest fires appear. The collapse of a sand pile, which is one kind of landslide, is a good example of an avalanche. Other than these, a very interesting avalanche, which is called a vortex avalanche and is much more complicated than any other, appears in superconductor. This was observed in type-two superconductors, such as MgB₂, Nb, Nb alloys, YNi₂B₂C, and YBCO thin film,¹⁻⁶ with vortices penetrating into the superconductor. This phenomenon is related to a number of physical quantities, such as the temperature, the critical current density, the thermal conductivity, the specific heat, the demagnetization factor, and so on.⁷⁻¹⁶ The avalanche phenomenon is known to show sudden change from gradual vortex penetration to chaotic vortex penetration, which is caused by a small perturbation in the parameters mentioned above.

In a fixed magnetic field, a dendritic arrangement shows up with temperature until the threshold temperature (T_I) is reached.⁹ Above T_I , the magnetic penetration becomes gradual, as is observed for quite a number of superconducting films. This situation is similar to that of a threshold magnetic field H_I .^{9,10} In other words, there exists a clear line of the vortex instability in the (H_I , T_I) plane, above which the dendritic patterns disappear, and the vortices are redistributed. Thus, a phase diagram of the magnetic instability can be drawn in the H - T plane.

Until now, quite a number of theories have been developed to explain the vortex avalanche phenomenon,¹¹⁻¹⁶ which critically depends on the parameters mentioned above.⁷⁻¹⁰ However, until now, the sweeping rate (SR) of the applied magnetic field has not been considered seriously. Changes in the ramping rate of the magnetic field are now possible because new vibrating superconducting quantum in-

terference device (SQUID) magnetometers have a capability of handling SRs up to 700 Oe/s, which is quite large, compared to previous dc SQUID magnetometers. Thus, in this research, we increased the SR of the applied magnetic field up to 500 Oe/s and studied the magnetic instability. In our experimental results, we observed different magnetic instability regions for different SRs of the magnetic field. Wider ranges of magnetic instability were obtained for higher SRs. Using the hysteresis loops, we were able to determine the (H_I , T_I) phase diagram for dendritic jumps in MgB₂ thin film for various SRs of the magnetic field.

II. EXPERIMENTS AND DISCUSSION

In this study, we prepared MgB₂ thin film by using a two-step method: pulse laser deposition (PLD) and post annealing.¹⁷ Using a PLD system, we synthesized the boron precursor film on a sapphire substrate and put it into a Nb tube with a pure piece of Mg. We then sealed the tube by using an arc melting method. In the Nb tube, the piece of Mg evaporated and reacted with the boron precursor film in an Ar atmosphere. The dimensions of sample were 2.3 mm × 2.5 mm × 500 nm.

Magnetic hysteresis loops were measured at fields from -5 to 5 T by using a SQUID-VSM (SQUID-vibrating sample magnetometer: Quantum Design) under different SRs. The lowest SR of the magnetic field was 3 Oe/s, and the highest SR was 500 Oe/s. The measurement temperature ranged from $T=2$ to 12 K in 0.3 to 1 K intervals. The temperature dependence of the low-field magnetization indicated that the superconducting transition temperature was 38 K.

In Fig. 1, we show the initial parts of the magnetic hysteresis loops at $T=6$ K. All results are shifted downward by 0.015 emu from the 3 Oe/s result for clear distinction of each curve. In Fig. 1(a), the height of the noise signal in the 3 Oe/s curve appears to be larger than it is in the other results but this is due to there being more data points at this SR than

^{a)}Electronic mail: silee77@sogang.ac.kr.

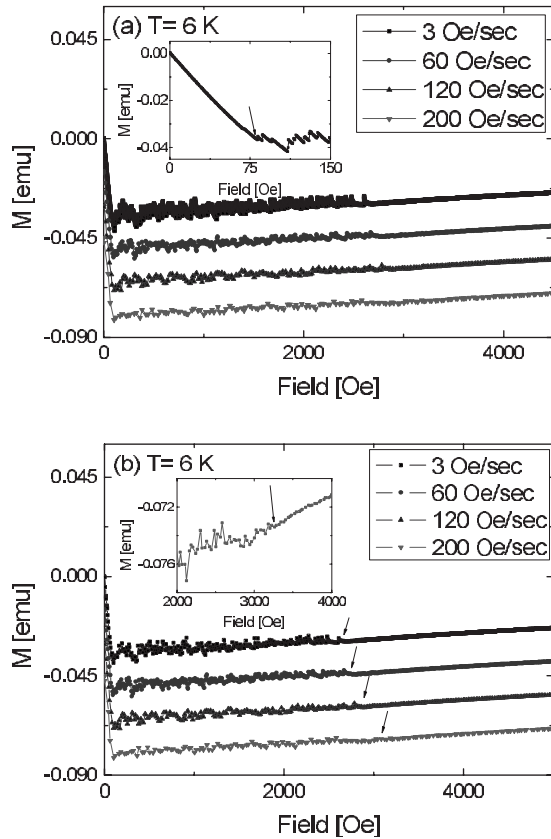


FIG. 1. Initial parts of the hysteresis loops. (a) all data and (b) data extracted for the 3 Oe/s SR to direct comparison. Black arrows are guides for finding the upper threshold field. The inset in (a) is an expanded part of the case of 3 Oe/s, and the arrow indicates the lower threshold field. The inset in (b) is an expanded part of the case of 200 Oe/s, and the arrow indicates the upper threshold field.

at higher SRs. Thus, we intentionally extracted data points in the 3 Oe/s case for a fair comparison with faster SRs and the results are shown in Fig. 1(b). In this picture, the heights of noise signal are more or less same for all SRs. The inset of Fig. 1(a) shows the lower threshold field in which flux noises appear as indicated by the arrow. Since there are fewer data points at higher SRs compared to 3 Oe/s, we did not determine the lower threshold field except for the lowest SR, as shown the inset of Fig. 1(a). Additionally, the upper threshold field for 200 Oe/s is shown in an expanded view in the inset of Fig. 1(b). These results show the noise region of the flux jumps is wider for a higher SR of the applied magnetic field than it is for a lower SR. In this experimental result, we conclude that at the same temperature, a fast ramping of the magnetic field produces an instability region that is wider than produced by a slow SR.

Figure 2 shows the initial parts of the magnetic hysteresis loops at (a) $T=10.8$ K and (b) 11 K. The temperature of 10.8 K is very near the phase boundary between flux stability and instability. Flux jumps appear at SRs of 120 and 200 Oe/s but not at 3 and 60 Oe/s, as shown in Fig. 2(a). This implies that the stability of the vortex avalanche critically depends on the ramping rate of the magnetic field. As shown in Fig. 2(b) for $T=11$ K, which is 0.2 K above the case of Fig. 2(a), a vortex avalanche does not appear no matter the SR, and all the vortex phases for any SR belong to the region of stable phases.

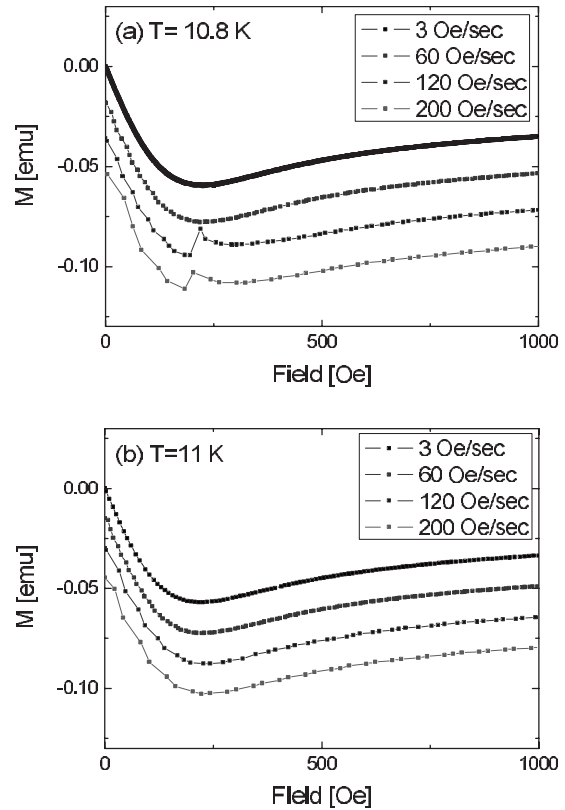


FIG. 2. Initial parts of the magnetic hysteresis loops under various magnetic field SRs at (a) 10.8 K and (b) 11 K. Except for the 3 Oe/s result, the other graphs are shifted down by 0.015 emu. At 11 K, flux jumps do not appear.

Based on these results, we drew a H - T phase diagram of the flux instability. The upper threshold fields which a flux jump ends were determined from the initial parts of the hysteresis curves. As explained before, the lower threshold field at which the magnetic flux noise first appears was obtained for 3 Oe/s for the temperature range between 2 and 10 K. Above 11 K, flux noise does not appear, no matter what the SR is. The Meissner phase in Fig. 3(a) was determined from the points that deviate from linearity in the initial part of the hysteresis loop for the 3 Oe/s case. From the M - H graphs, we found the Meissner regions to be the same for different SRs. A small gap exists between the lower threshold field and the lower critical field, and this result implies that a dendritic jump appears above a certain range of the magnetic field. In this gap, the magnetic field penetrates without a dendritic flux jump but above this gap, moving vortices induce an unstable vortex avalanche in the superconducting film. In this graph, the instability phase region becomes quite wide at the higher SRs. The increase in the upper threshold field for the highest SR is about two times compared to that for the lowest SR at $T=2$ and 4 K. In Fig. 3(b), we show the temperature dependence of the SR, which obtained by using the results in Fig. 3(a). Under the same upper threshold field, we chose four points of the SR while extrapolating the data points in Fig. 3(a). The left side of each point under the same upper threshold field is the flux-jump state and the right side is a stable state. The SR value which clearly causes the flux jump increase very rapidly with the small increasing temperature. This fast increase becomes much slower for larger

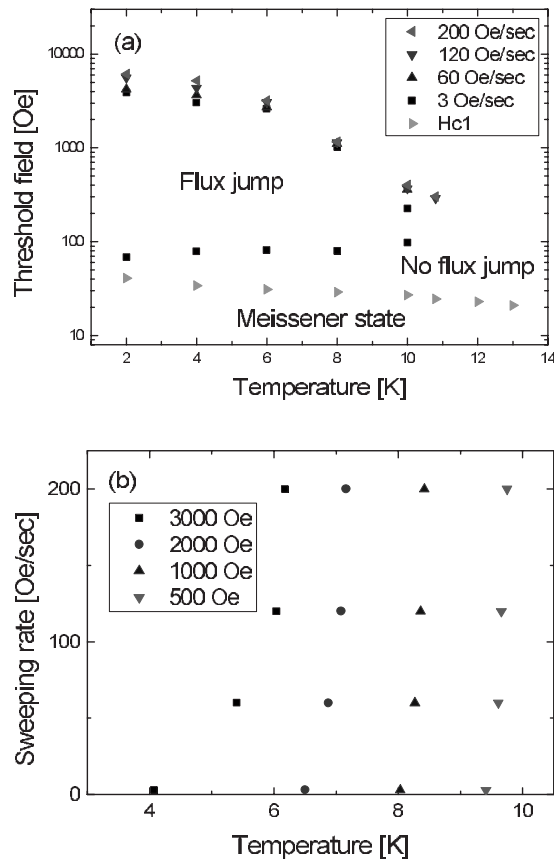


FIG. 3. (a) Temperature-magnetic field phase diagram. (b) Temperature dependence of the SR under a finite upper threshold field. The left side of a point is the flux-jump region and the right side is the no-flux-jump region.

upper threshold field values, which means that the intervals between SR results become smaller at higher temperatures. In this graph, we clearly see that the flux-jump state critically depends on the SR of the applied magnetic field and that the upper limit for the disappearance of the flux jumps can be obtained from the temperature axis.

This increase in the flux noise region for faster SRs is also observed for the remnant parts of the hysteresis loops, as shown in Fig. 4. The flux unstable region is seen to become a little bit wider for the remnant part than that for the initial part. For example, at 11 K, flux noise appears in the remnant part of hysteresis loop in Fig. 4(b) but does not appear in the initial part shown in Fig. 2(b). This may originate from the additional heat generated by the flux and anti-flux recombination in the remnant part of hysteresis loops.¹⁰ Thus, the region of unstable flux jumps is hysteric dependent.

It is time to explain why a vortex avalanche depends on the SR. To explain our experimental result, we consider the following possible origin. The shielding current in a thin film is increased by increasing the applied magnetic field. If the SR of the applied magnetic field increases, then the shielding current in a superconductor also increases under a same time interval. Once vortices penetrate into the superconducting thin film, Joule heat is generated by the coupling between the moving vortices and the current. However, at higher SRs, the thin film does not have enough time to dissipate the Joule heat to recover the superconducting state and induce a posi-

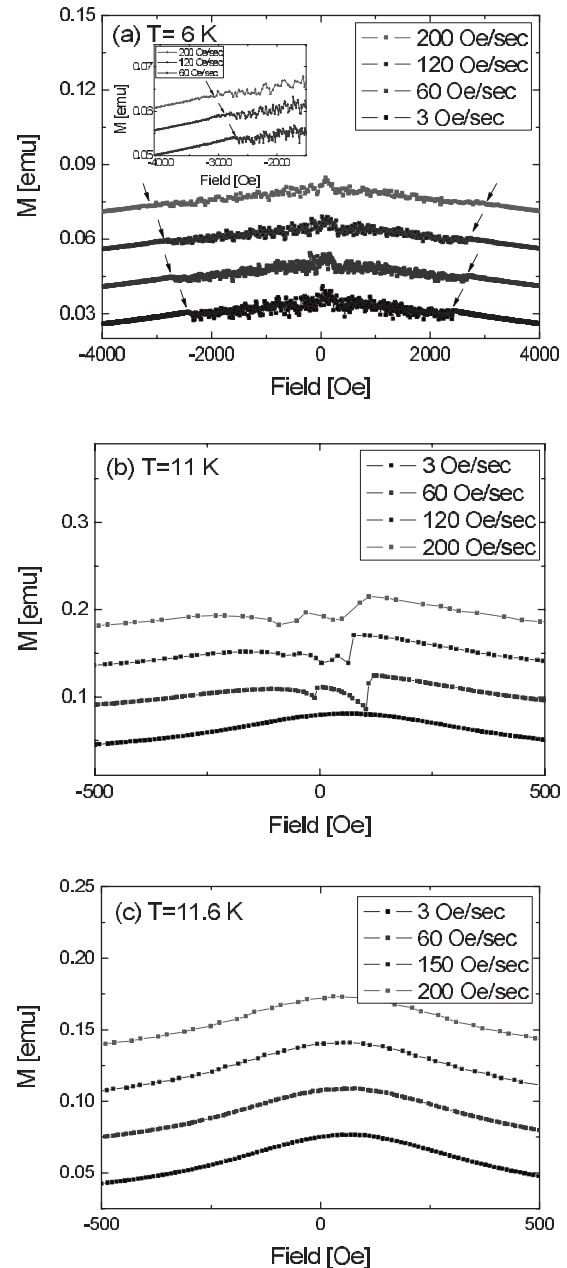


FIG. 4. Remnant parts of the magnetic hysteresis loops at (a) $T=6$ K, (b) $T=11$ K, and (c) $T=11.6$ K.

tive feedback effect which makes a vortex avalanche. But under slow SRs, this is not the case because the superconducting thin film has enough time to dissipate Joule heat. Also the background electric field is increased by a relation between the background electric field and the SR, which can be expressed as $E \sim l dH/dt$, where l is the half width of the sample.^{14,15} In this case, the flux flow resistivity also increases because E is proportional to the flux flow resistivity ρ_F .^{18,19} Accordingly, the ratio between the thermal and the magnetic diffusion time decreases with increasing flux flow resistivity and a positive feedback effect also induces a vortex avalanche.^{11,12} Since the vortex avalanche becomes very sensitive to external parameters near the stable-unstable phase boundary, a small change in an external parameter, such as the SR of magnetic field, becomes critical for the vortex avalanche.

III. CONCLUSIONS

In summary, we studied the temperature dependence of the vortex avalanche under various SRs of the magnetic field. Noises from dendritic propagation are affected by the SR, and a faster SR shows a wider region of unstable phase. Even for the same temperature near the phase boundary, flux jumps appear only at faster SRs, not at a slow SRs. Based on above results, we have drawn a phase diagram of stable and unstable vortex phases as well as the Meissner phase in the H - T plane for various SRs. Our results show that near the phase boundary, the vortex avalanche is indeed critically affected by small changing in the SR.

ACKNOWLEDGMENTS

This work was supported by the Center for Superconductivity of the program of Acceleration Research of MOST/KOSEF of Korea (Contract No. 2009-0051705) and by a special fund from Sogang University.

- ¹I. A. Rudnev, S. V. Antonenko, D. V. Shantsev, T. H. Johansen, and A. E. Primenko, *Cryogenics* **43**, 663 (2003).
²S. C. Wimbush, B. Holzapfel, and Ch. Jooss, *J. Appl. Phys.* **96**, 3589 (2004).
³I. A. Rudnev, D. V. Shantsev, T. H. Johansen, and A. E. Primenko, *Appl. Phys. Lett.* **87**, 042502 (2005).
⁴Z. W. Zhao, S. L. Li, Y. M. Ni, H. P. Yang, Z. Y. Liu, H. H. Wen, W. N. Kang, H. J. Kim, E. M. Choi, and S. I. Lee, *Phys. Rev. B* **65**, 064512 (2002).

- ⁵T. H. Johansen, M. Baziljevich, D. V. Shantsev, P. E. Goa, Y. M. Galperin, W. N. Kang, H. J. Kim, E. M. Choi, M.-S. Kim, and S. I. Lee, *Europhys. Lett.* **59**, 599 (2002).
⁶P. Leiderer, J. Boneberg, P. Brull, V. Bujok, and S. Herminghaus, *Phys. Rev. Lett.* **71**, 2646 (1993).
⁷E.-M. Choi, H.-S. Lee, H.-J. Kim, S.-I. Lee, H.-J. Kim, and W. N. Kang, *Appl. Phys. Lett.* **84**, 82 (2004).
⁸E.-M. Choi, H.-S. Lee, H.-J. Kim, B.-W. Kang, S.-I. Lee, A. A. F. Olsen, D. V. Shantsev, and T. H. Johansen, *Appl. Phys. Lett.* **87**, 152501 (2005).
⁹J.-Y. Lee, E.-M. Choi, H.-S. Lee, M.-H. Cho, A. A. F. Olsen, T. H. Johansen, Y. S. Oh, K.-H. Kim, Y.-H. Han, T. H. Sung, and S.-I. Lee, *J. Phys. Soc. Jpn.* **77**, 104717 (2008).
¹⁰E.-M. Choi, H.-S. Lee, J.-Y. Lee, S.-I. Lee, A. A. F. Olsen, V. V. Yurchenko, D. V. Shantsev, T. H. Johansen, H.-J. Kim, and M.-H. Cho, *Appl. Phys. Lett.* **91**, 042507 (2007).
¹¹D. V. Denisov, D. V. Shantsev, Y. M. Galperin, E.-M. Choi, H.-S. Lee, S.-I. Lee, A. V. Bobyl, P. E. Goa, A. A. F. Olsen, and T. H. Johansen, *Phys. Rev. Lett.* **97**, 077002 (2006).
¹²I. Aranson, A. Gurevich, M. Welling, R. Wijngaarden, V. Vlasko-Vlasov, V. Vinokur, and U. Welp, *Phys. Rev. Lett.* **94**, 037002 (2005).
¹³D. V. Shantsev, A. V. Bobyl, Y. M. Galperin, T. H. Johansen, and S. I. Lee, *Phys. Rev. B* **72**, 024541 (2005).
¹⁴D. V. Denisov, A. L. Rakhmanov, D. V. Shantsev, Y. M. Galperin, and T. H. Johansen, *Phys. Rev. B* **73**, 014512 (2006).
¹⁵A. L. Rakhmanov, D. V. Shantsev, Y. M. Galperin, and T. H. Johansen, *Phys. Rev. B* **70**, 224502 (2004).
¹⁶F. L. Barkov, D. V. Shantsev, T. H. Johansen, P. E. Goa, W. N. Kang, H. J. Kim, E. M. Choi, and S. I. Lee, *Phys. Rev. B* **67**, 064513 (2003).
¹⁷H.-J. Kim, W. N. Kang, E.-M. Choi, M.-S. Kim, K. H. P. Kim, and S.-I. Lee, *Phys. Rev. Lett.* **87**, 087002 (2001).
¹⁸I. Aranson, A. Gurevich, and V. Vinokur, *Phys. Rev. Lett.* **87**, 067003 (2001).
¹⁹E. H. Brandt, *Phys. Rev. B* **52**, 15442 (1995).